Theoretical Study of Silyl-Bridged Dinuclear Palladium(I) and Platinum(I) Complexes, $M_2(\mu\text{-}\eta^2\text{-}H\cdots SiH_2)_2(PH_3)_2$ (M = Pd or Pt). New Insight into the Bonding Nature

Shingo Nakajima,[†] Michinori Sumimoto,[†] Yoshihide Nakao,[†] Hirofumi Sato,[†] Shigeyoshi Sakaki,*[,†,‡] and Kohtaro Osakada[§]

Department of Molecular Engineering, Graduate School of Engineering, Kyoto University, Nishikyo-ku, Kyoto 615-8510 Japan, Fukui Institute for Fundamental Chemistry, Kyoto University, Sakyo-ku, Kyoto 606-8501, Japan, and Chemical Resources Laboratory, Tokyo Institute of Technology, 4259 Nagatsuda, Midori-ku, Yokohama 226-8503, Japan

Received April 17, 2005

Silyl-bridged dinuclear palladium(I) and platinum(I) complexes with the composition $M_2(SiH_3)_2(PH_3)_2$ (M = Pd or Pt) were theoretically investigated with DFT, MP2 to MP4(SDQ), and CCSD(T) methods. These complexes are more stable than two $M(PH_3)(SiH_3)$ complexes by 80.6 kcal/mol for M = Pd and 105.6 kcal/mol for M = Pt, where the values calculated with the CCSD(T) method are given hereafter. Although this complex is understood to take the silyl-bridged form in a formal sense, the NMR chemical shifts of Si and H atoms and the Laplacian of electron density indicate that the electronic structure of the SiH_3 group somewhat shifts toward that of the silylene + hydride groups and the agostic interaction is responsible for this interesting electronic structure. These complexes are represented as $M_2(\mu\text{-}\eta^2\text{-}H\cdots SiH_2)_2(PH_3)_2$, in which the formula of $H\cdots SiH_2$ indicates that this group is not a pure silyl group but possesses the characteristics of the hydride and μ-silylene groups to a considerable extent. The planar geometry of this compound comes from the presence of the three-center two-electron (3c-2e) interaction between the silyl sp^3 orbital and the M−M moiety, while these complexes become nonplanar in the absence of the 3c-2e interaction. The agostic interaction between the Si−H bond and the M center contributes to the stabilization energies of 8.0 and 17.3 kcal/mol for M = Pd and Pt, respectively. The stronger agostic interaction and the larger stabilization energy of $Pt_2(\mu\text{-}\eta^2\text{-}H\cdots SiH_2)_2(PH_3)_2$ than those of the Pd analogue result from the fact that the d orbital of Pt expands more than that of Pd.

Introduction

Primary (SiH_3R) and secondary (SiH_2R_2) organosilanes react with transition metal complexes to afford a variety of products,[1] as shown in Scheme 1. For instance, various $\mu\text{-}\eta^2$-$HSiR_2$- and $\mu\text{-}\eta^2$-HSiHR-bridged dinuclear Pd(I) and Pt(I) complexes (Scheme 1(B)) were reported as products of the reactions of primary and secondary silanes with Pd(0) and Pt(0) complexes.[2−4] Also, similar $\mu\text{-}\eta^2$-silyl-bridged Rh(II)[5] and Ru(I)[6,7] dinuclear complexes and $\mu\text{-}\eta^2$-silyl-bridged heterodinuclear Pd(I) and Pt(I) complexes[8] were reported, so far.

These complexes have drawn a lot of attention because some of them are key intermediates of transformation reactions of silane mediated by transition metal complexes and some of them contain interesting

* To whom correspondence should be addressed. E-mail: sakaki@moleng.kyoto-u.ac.jp.
† Department of Molecular Engineering, Kyoto University.
‡ Fukui Institute for Fundamental Chemistry, Kyoto University.
§ Tokyo Institute of Technology.

(1) (a) Schubert, U. *Adv. Organomet. Chem.* **1990**, *30*, 151. (b) Tobita, H.; Ogino, H. *Adv. Organomet. Chem*. **1998**, *42*, 223. (c) Corey, J.-Y.; Braddock-Wilking, J. *Chem. Rev.* **1999**, *99*, 175. (e) Braunstein, P.; Boag, N. M.; *Angew. Chem., Int. Ed.* **2001**, *40*, 2427.
(2) Auburn, M.; Ciriano, M.; Howard, J. A. K.; Murray, M.; Pugh, N. J.; Spencer, J. L.; Stone, F. G. A.; Woodward, P. *J. Chem. Soc., Dalton Trans.* **1980**, 659.
(3) (a) Kim, Y.-J.; Lee, S.-C.; Park, J.-I.; Osakada, K.; Choi, J.-C.; Yamamoto, T. *Organometallics* **1998**, *17*, 4929. (b) Kim, Y.-J.; Lee, S.-C.; Park, J.-I.; Osakada, K.; Choi, J.-C.; Yamamoto, T. *J. Chem. Soc., Dalton Trans.* **2000**, 417. (c) Tanabe, M.; Yamada, T.; Osakada, K. *Organometallics* **2003**, *22*, 2190.
(4) (a) Levchinsky, Y.; Rath, N. P.; Braddock-Wilking, J. *Organometallics* **1999**, *18*, 2583. (b) Sanow, L. M.; Chai, M.; McConnville, D. B.; Galat, K. J.; Simone, R. S.; Rinaldi, P. L.; Youngs, W. J.; Tessier, C. D. *Organometallics* **2000**, *19*, 192. (c) Braddock-Wilking, J.; Levchinsky, Y.; Rath, N. P. *Organometallics* **2000**, *19*, 5500. (d) Braddock-Wilking, J.; Levchinsky, Y.; Rath, N. R. *Organometallics* **2001**, *20*, 474. (e) Braddock-Wilking, J.; Corey, J. Y.; Dill, K.; Rath, N. P. *Organometallics* **2002**, *21*, 5467. (f) Braddock-Wilking, J.; Corey, J. Y.; Tranker, K. A.; Dill, K. M.; Frenck, L. M.; Rath. N. P. *Organometallics* **2004**, *23*, 4576.
(5) (a) Fryzuk, M. D.; Rosenberg, L.; Rettig, S. J. *Organometallics* **1991**, *10*, 2537. (b) Fryzuk, M. D.; Rosenberg, L.; Rettig, S. J. *Inorg. Chim. Acta* **1994**, *222,* 345. (c) Fryzuk, M. D.; Rosenberg, L.; Rettig, S. J. *Organometallics* **1996**, *15*, 2871. (d) Rosenberg, L.; Fryzuk, M. D.; Rettig, S. J. *Organometallics* **1999**, *18*, 958.
(6) (a) Suzuki, H.; Takao, T.; Tanaka, M.; Moro-oka, T. *J. Chem. Soc., Chem. Commun.* **1992**, 476. (b) Takao, T.; Toshida, S.; Suzuki, H.; Tanaka, M. *Organometallics* **1995**, *14*, 3855.
(7) (a) Hashimoto, H.; Hayashi, Y.; Aratani, I.; Kabuto, C.; Kira, M. *Organometallics* **2002**, *21*, 1534. (b) Hashimoto, H.; Hayashi, Y.; Aratani, I.; Kabuto, C.; Kira, M. *Organometallics* **2003**, *22*, 2199.
(8) Tanabe, M.; Osakada, K. *Inorg. Chim. Acta* **2003**, *350*, 201.

10.1021/om050292i CCC: $30.25
Publication on Web 07/09/2005

Scheme 1[a]

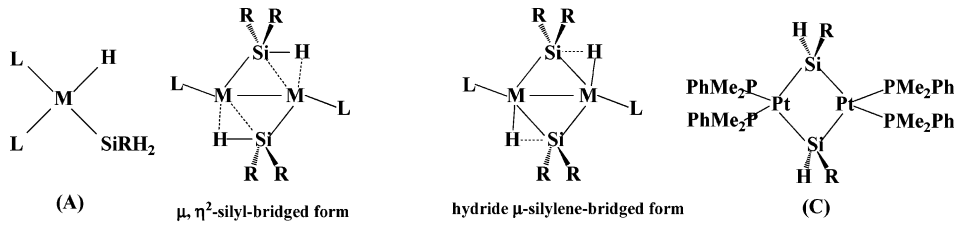

[a] M = Pd or Pt.

bonding nature and geometries.[1] For instance, the μ-η^2-silyl-bridged dinuclear Pd(I) and Pt(I) complexes contain a nonclassical three-center two-electron (3c-2e) interaction between the μ-η^2-silyl group and the M−M moiety,[1a,c,9] as shown in Scheme 1(B-1). However, there is the other plausible way to understand this complex in terms of a hydride μ-silylene-bridged form in which the H(hydride) ligand coordinates with the Pd center and also interacts with the empty p orbital of the bridging μ-silylene group, as shown in Scheme 1(B-2). This bonding feature is considered reasonable because the singlet silylene is electron-acceptable due to the presence of the empty p orbital and can form a charge-transfer interaction with the electron-rich hydride ligand. Actually, the considerably long Si−H distances were experimentally reported in $Pd_2(\mu\text{-}SiHPh_2)_2(PMe_3)_2$ and the Pt analogues.[3a,b,4a,c] These long Si−H distances experimentally suggest that these complexes take the hydride μ-silylene-bridged form. Thus, it is interesting to investigate which understanding is correct. Besides this issue, there remain several important issues to be investigated in detail, as follows: The first issue is the planar M_2Si_2 moiety. In the silyl-bridged dinuclear Rh(II) complex with the composition $Rh_2(H)_2(SiH_3)_2(PR_3)_2$, the Rh_2Si_2 moiety is not planar but the dihedral angle between two Rh−Rh−Si planes is 74.5°.[5d] It is worthwhile to clarify the reason for the planar geometry of $Pd_2(\mu\text{-}SiHPh_2)_2(PMe_3)_2$ and the Pt analogues. Also, it is important how the 3c-2e and agostic interactions are formed in these complexes and how much they contribute to the stabilization of these complexes.

Despite the interesting issues mentioned above, these complexes have not been theoretically investigated well except for one pioneering work.[9a] In this previous study, the 3c-2e interaction was discussed in detail based on the Laplacian of electron density. However, no discussion was presented to show how much the 3c-2e and agostic interactions participate in the geometry and bonding nature of these complexes.

In the present study, μ-η^2-SiH_3-bridged dinuclear Pd(I) and Pt(I) complexes with the composition $M_2(SiH_3)_2(PH_3)_2$ (M = Pd or Pt) were theoretically investigated as a model of $M_2(HSiR_2)_2(PH_3)_2$ (R = aryl, etc.) with the DFT, MP2 to MP4(SDQ), and CCSD(T) methods. Our main purposes here are to clarify the electronic structure and the bonding nature of these complexes, in particular, to show whether the μ-η^2-silyl-bridged form or the hydride μ-sylilene-bridged form is the correct understanding, how the 3c-2e and agostic interactions are formed in $M_2(SiH_3)_2(PH_3)_2$, and how much these interactions play important roles to determine the geometry and the bonding nature of these dinuclear complexes. In our previous work, we found significant differences between μ-disilene-bridged dinuclear Pd(0) and bis(μ-silylene)-bridged dinuclear Pt(0) complexes.[10] Thus, it is also our purpose to show the differences and similarities between $Pd_2(SiH_3)_2(PH_3)_2$ and the Pt analogue, and to elucidate the reasons.

Computations

Geometries were optimized by the DFT method with the B3LYP functional.[11,12] We ascertained that the optimized geometries did not exhibit any imaginary frequency except for the geometries that were optimized under some constraints. Energy and population changes were evaluated with the DFT, MP2 to MP4(SDQ), and CCSD(T) methods. In the CCSD(T) calculation, the contribution of triple excitations was incorporated noniteratively with single and double excitation wave functions.[13]

The basis set system described below was mainly used for the calculation. For Pd, the MIDI-4 basis set was used,[14] where one diffuse d function (ζ = 0.124)[15] was added and the 5p orbitals were represented by the same exponents and the same coefficients as those of the 5s orbital.[15] For Si, the Huzinage−Dunning (11s7p1d)/[6s4p1d] basis set was used.[18] For P, a (21/21/1) basis set was employed for the valence electrons,[19] where core electrons of P (up to 2p) were replaced with the effective core potentials (ECPs) and one d-polarization function was added.[20] For H, the 6-311G basis set was employed, where a p-polarization function was added for the H atoms of the silyl

(9) (a) Choi, S.-H.; Lin, Z. *J. Organomet. Chem.* **2000**, *608*, 42. (b) Lin, Z. *Chem. Soc. Rev.* **2002**, *31*, 239.

(10) (a) Sakaki, S.; Yamaguchi, S.; Musashi, Y.; Sugimoto, M. *J. Organomet. Chem.* **2001**, *635*, 173. (b) Nakajima, S.; Yokogawa, D.; Nakao, Y.; Satp, H.; Sakaki, S.; *Organometallics* **2004**, *23*, 4672.

(11) (a) Becke, A. D. *Phys. Rev. A* **1988**, *38*, 3098. (b) Becke, A. D. *J. Chem. Phys.* **1983**, *98*, 5648.

(12) Lee, C.; Yang, W.; Parr, R. G. *Phys. Rev. B* **1988**, *37*, 785.

(13) (a) Purvis, G. D., III; Bartlett, R. J. *J. Chem. Phys.* **1982**, *76*, 1910. (b) Raghavachari, K.; Trucks, G. W.; Pople, J. A.; Head-Gordon, M. *Chem. Phys. Lett.* **1989**, *157*, 479.

(14) Huzinaga, S.; Andzelm, J.; Klobukowski, M.; Radzio-Andzelm, E.; Sakai, Y.; Tatewaki, H. *Gaussian basis sets for molecular calculations*; Elsevier: Amsterdam, 1984.

(15) One d function was added to represent well the d electron, the exponent of which was determined with an even-tempered criterion.

(16) (a) When we used two p functions provided as standard polarization functions of MIDI-4,[14] the optimized Pd−Pd distance is considerably longer than the experimental value (see Supporting Information Table S1). The standard LANL2DZ basis set[17] of Pd also presented somewhat longer Pd−Pd and Pd−P distances, where one f-polarization function was added[16b] (see also Supporting Information Table S1). (b) Ehlers, A. W.; Böhme, M.; Dapprich, S.; Gobbi, A.; Höllwarth, A.; Jonas, V.; Köhler, K. F.; Stegmann, R.; Veldkamp, A.; Frenking, G. *Chem. Phys. Lett.* **1993**, *208*, 111.

(17) Hay, P. J.; Wadt, W. R. *J. Chem. Phys.* **1985**, *82*, 299.

(18) Dunning, T. M., Jr.; Hay, P. J. In *Methods of Electronic Structure Theory*; Schaeffer, H. F., III, Ed.; Plenum: New York, 1977; p 1.

(19) Wadt, W. R.; Hay, P. J. *J. Chem. Phys.* **1985**, *82*, 284.

(20) Höllwarth, A.; Böhme, M.; Dapprich, S.; Ehlers, A. W.; Gobbi, A.; Jonas, V.; Köhler, K. F.; Stegmann, R.; Veldkamp, A.; Frenking, G. *Chem. Phys. Lett.* **1993**, *208*, 237.

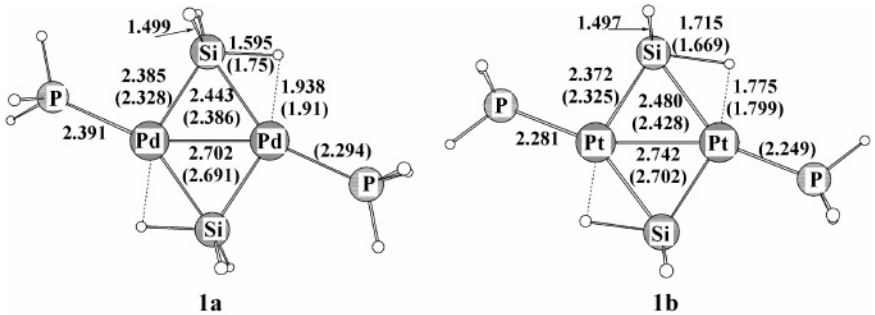

Figure 1. Optimized geometries of $Pd_2(SiH_3)_2(PH_3)_2$ **1a** and the Pt analogue **1b**. Bond distances in angstroms and bond angles in degrees. In parentheses are experimental values.[3,4a]

group.[21] We used this basis set system for geometry optimization and evaluation of energy changes. In the calculations of NMR chemical shifts, basis sets for Si, P, and H were changed to the 6-311+G(d,p) basis sets[22] without any change for the other atoms, where a diffuse function was eliminated from the basis set used for P. This basis set system was selected after NMR chemical shifts were evaluated with various basis set systems (see Supporting Information Table S2). For Pt, the standard LANL2DZ basis set[17] was used for geometry optimization, where the basis sets and ECPs for the other atoms were taken to be the same as those employed for the Pd system. The optimized geometry of $Pt_2(SiH_3)_2(PH_3)_2$ with this basis set system agrees with the experimental one, as will be discussed below. The better (541/541/111) basis set[17,23] was employed for Pt with the same ECPs as LANL2DZ to evaluate energy changes and electron distribution, while the basis sets for the other atoms were not changed. When the electron distribution was compared between Pd and Pt complexes, the (541/541/211) basis set and ECPs[17,23] were employed for Pd to make the comparison with the basis sets of the same quality.

The Gaussian 98 program package was used for these calculations.[24] NMR chemical shifts were evaluated with the GIAO method[25] at the DFT level. Population analysis was carried out with the method of Weinhold et al.[26] The contour map of molecular orbitals was drawn with the Molden program package.[27] We employed here simple model compounds, $M_2(SiH_3)_2(PH_3)_2$, because the geometry of the M_2Si_2 flame is similar in the model and real compounds, as will be described below.[28]

Results and Discussion

Geometrical Features of $M_2(SiH_3)_2(PH_3)_2$. Optimized geometries of $Pd_2(SiH_3)_2(PH_3)_2$ **1a** and the Pt analogue **1b** are shown in Figure 1. The Pd−Pd distance agrees well with the experimental value.[3] Although the Pd−Si distances (2.385 and 2.443 Å) are moderately longer than the experimental values (2.328 and 2.386 Å), the difference between two Pd−Si distances is well reproduced by the present computation. The Pd−H distance agrees well with the experimental value, too. It is noted that the optimized Si−H bond is much shorter than the experimental value. However, this discrepancy in the Si−H bond between computational and experimental results does not mean that the computational results are not reliable because the position of the H atom is not experimentally determined very well, in general.[29] In the Pt analogue **1b**, the optimized Pt−Pt distance and the Pt−Si distances (2.742 and 2.480 Å) agree with the experimental values.[4a] The Pt−H distance agrees well with the experimental value, while the Si−H distance somewhat deviates from the experimental value like that of the Pd analogue.[29] Although the Pd−P distance is overestimated by the computation, the fundamental geometrical features of the $M_2Si_2H_2$ moiety[3,4a] are reproduced well by the present computations in both the Pd and Pt complexes.[30]

The optimized Si−H bond distance is longer than the usual Si−H bond. This result suggests that the Si−H bond of the μ-η^2-silyl group forms an agostic interaction with the M center. It should be noted here that the Pd−H distance is much longer than the Pt−H distance in both experimental[3,4a] and computational geometries and that the optimized Si−H distance of **1b** is much longer than that of **1a**. These results suggest that the agostic interaction is stronger in the Pt complex than in the Pd complex. Their bonding nature will be discussed below in detail.

The Pt−Pt−P and Pd−Pd−P angles are not 180° but about 155°. The P−M−Si angle is 99° and 101°, the M−M−Si angle is 55° and 54°, the M−M−H angle is 96° and 98°, and the P−M−H angle is 109° and 104° for M = Pd and Pt, respectively (see Supporting Information Figure S2). Because the Pt and Pd atoms have d^9 electron configuration in these complexes, the

(21) Duning, T. H. *J. Chem. Phys.* **1971**, *55*, 716. Hehre, W. J.; Radom, L.; Schleyer, P. v. R.; Pople, J. A. *Ab Initio Molecular Orbital Theory*; John Wiley & Sons: New York, 1986; p 82.

(22) McLean, A. D.; Chandler, G. S. *J. Chem. Phys.* **1980**, *72*, 5639.

(23) Couty, M.; Hall, M. B. *J. Comput. Chem.* **1996**, *17*, 1359.

(24) Pople, J. A.; et al. *Gaussian 98*; Gaussian Inc.: Pittsburgh, PA, 1998.

(25) (a) McWeeny, R. *Phys. Rev.* **1962**, *126*, 1028. (b) Ditchfield, R. *Mol. Phys.* **1974**, *27*, 789. (c) Dodds, J. L.; McWeeny, R.; Saldej, A. J. *Mol. Phys.* **1980**, *41*, 1419. (d) Walinski, K.; Hilton, J. F.; Pulay, P. *J. Am. Chem. Soc.* **1990**, *112*, 8251.

(26) Reed, A. E.; Curtis, L. A.; Weinhold, F. *Chem. Rev*. **1988**, *88*, 849, and references therein.

(27) Schaftenaar, G..; Noordik, J. H. *J. Comput.-Aided Mol. Des.* **2000**, *14*, 123.

(28) We optimized real compound $Pd_2(\mu$-η^2-$SiHPh_2)_2(PMe_3)_2$ with the DFT method, where the LANL2DZ basis set was used for Pd (see Supporting Information Figure S1). However, the optimized geometry of the Pd_2Si_2 flame rather deviates from the experimental one. This is probably because the DFT method does not incorporate well the dispersion interaction and overestimates the steric repulsion between the phenyl group and PMe_3. Thus, we decided to employ the model system here because the optimized geometry of the model system reproduces well the geometrical features of the Pd_2Si_2 flame; although the MP2 method incorporates the dispersion interaction, the MP2 optimization of the real compound is very time-consuming.

(29) In the experimental geometries, the Si−H distance of the Pt complex is somewhat shorter than that of the Pd complex by 0.08 Å.[3,4a] On the other hand, the Pd−H distance is much longer than the Pt−H distance,[3,4a] which indicates that the agostic interaction is stronger in the Pt complex than in the Pd analogue. These results are not consistent with each other, because the stronger agostic interaction leads to the longer Si−H distance in general. It is likely that the experimentally reported Si−H distance (1.75 Å) of the Pd complex is too long.

(30) Although the same compound was previously optimized,[9a] the optimized geometry presented here is much better than the previously reported one.

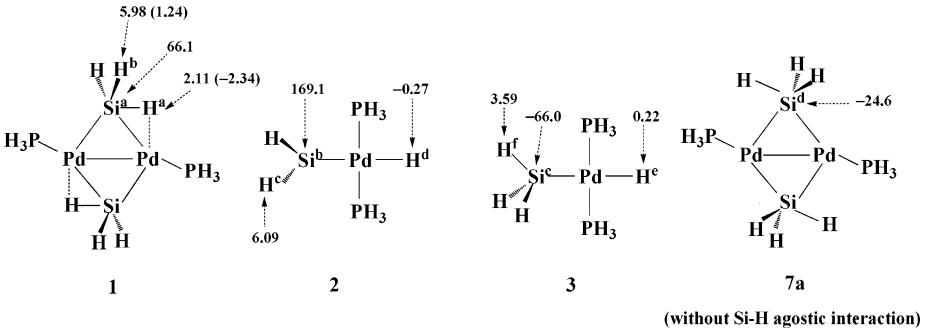

Figure 2. DFT-calculated NMR chemical shifts of $Pd_2(SiH_3)_2(PH_3)_2$ **1**, *trans*-$Pd(H)(SiH_2)(PH_3)_2$ **2**, *trans*-$Pd(H)(SiH_3)(PH_3)_2$ **3**, and $Pd_2(SiH_3)_2(PH_3)_2$ **7a** without agostic interactions.

Scheme 2

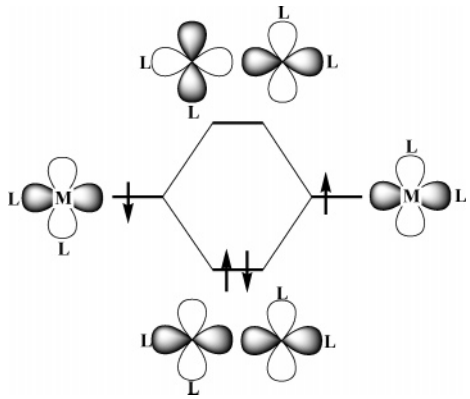

singly occupied d_σ orbital forms a σ-bond between two M centers, as schematically shown in Scheme 2. If we count the agostic interaction of the Si−H bond as one coordinate bond, one M center possesses one M−M bond, one agostic interaction, a M−PH_3 bond, and the M−Si bond. Thus, these complexes are understood to take a distorted four-coordinate structure around the M center, as discussed previsouly.[9]

NMR Chemical Shift of $Pd_2(SiH_3)_2(PH_3)_2$. To investigate whether the μ-η^2-silyl-bridged form or the μ^2-silylene hydride one is the correct understanding of this complex, we evaluated the NMR chemical shifts of H and Si atoms of **1a** and compared their chemical shifts with those of a model hydride silylene complex, *trans*-$Pd(H)(SiH_2)(PH_3)_2$, **2**, and a model hydride silyl complex, *trans*-$Pd(H)(PH_3)_2(SiH_3)$, **3**; see Supporting Information Figure S3 for their optimized geometries. Usually, the calculated value of the NMR chemical shift considerably depends on the basis sets. However, the chemical shifts of H and Si atoms of these compounds do not depend very much on the basis sets used here (Supporting Information Table S2). Although the calculated chemical shifts of H^a and H^b of **1a** are moderately larger than the experimental values, as shown in Figure 2, the difference between calculated chemical shifts (3.87 ppm) of H^a and H^b is almost the same as the experimental difference (3.58 ppm),[3a] where H^a, Si^a, etc., are defined in Figure 2. Interestingly, the chemical shift of H^a is intermediate between those of H^d and H^f, which are the hydride ligand and the H atom of the silyl ligand in **2** and **3**, respectively. Also, it is noted that the chemical shift of H^b is similar to that of H^c of SiH_2 in **2**, and the chemical shift of Si^a is almost intermediate between those of Si^b and Si^c, which are the Si atoms of SiH_2 and SiH_3 groups, respectively (see **2** and **3** in Figure 2). These results clearly indicate that the SiH_3 group of $Pd_2(SiH_3)_2(PH_3)_2$ is not a pure silyl group, but its Si atom is intermediate between those of silyl and silylene groups and the H^a atom is also intermediate between the usual H atom and the hydride ligand. More interestingly, the calculated NMR chemical shift of Si^d is −24.6 ppm in $Pd_2(\mu\text{-}SiH_3)_2(PH_3)_2$ (**7a**), in which the agostic interaction is not involved.[31] This value is rather similar to that of the silyl group of **3** but much different from that of **1a**. These results lead us to the conclusion that the agostic interaction of the Si−H bond is responsible for the characteristic features of the Si^a and H^a in **1a**.

On the other hand, the occupation number of the Si−H bond that forms the agostic interaction is 1.883e in **1a**. This value is not very much different from that (1.989e) of the usual Si−H bond. Moreover, the optimized Si−H distance is moderately longer than the usual Si−H bond, as mentioned above. Thus, it is likely that the Si−H bond is kept in $Pd_2(SiH_3)_2(PH_3)_2$ but the electronic structures of the Si and H atoms considerably shift toward those of the silylene group and the hydride ligand, respectively, due to the agostic interaction. All these results indicate that this compound should be described as $Pd_2(\mu\text{-}\eta^2\text{-}H\cdots SiH_2)_2(PH_3)_2$, in which the formula of $H\cdots SiH_2$ represents that the μ-η^2-$H\cdots SiH_2$ group is not a pure silyl group but possesses the characteristics of the hydride and μ-silylene group to a considerable extent.

The NMR chemical shift of Si^a of **1a** is understood, as follows: Because the Si−H bond becomes longer by the agostic interaction, the Si−H σ^* orbital becomes lower in energy. This Si−H σ^* orbital at low energy plays a similar role to that of the empty p orbital of the silylene moiety.

In the Pt complex **1b**, the optimized Si−H bond is much longer than that of the Pd complex **1a**. The occupation number (1.765) of the Si−H bond that participates in the agostic interaction is much smaller than that of **1a**. These features suggest that the electronic structure of the SiH_3 group shifts more toward the silylene and hydride groups in **1b** than in **1a**. Thus, NMR chemical shifts of **1b** are interesting and should be experimentally investigated in detail; however, the NMR chemical shifts of the Pt analogue could not be calculated here because the nonrelativistic calculation

(31) In **7a**, the silyl group is rotated by 180°, so that the H atom does not take a position close to the Pd center. A detailed discussion is given below in the section of the energy contribution of the agostic interaction.

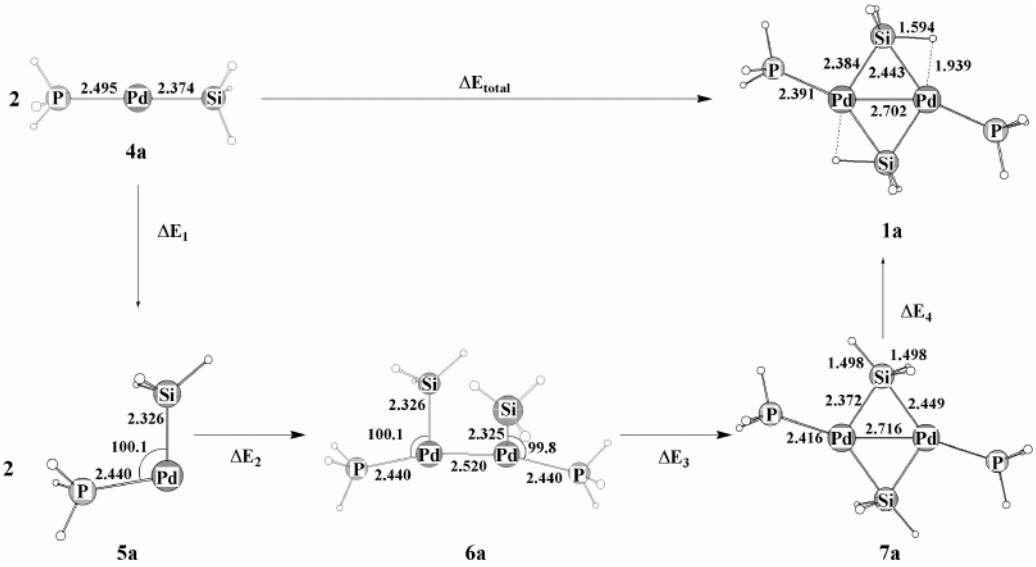

Figure 3. Geometry change along the assumed reaction from $Pd(SiH_3)(PH_3)$ to $Pd_2(SiH_3)_2(PH_3)_2$. Bond distances in angstroms and bond angles in degrees.

with all-electron basis sets is not reliable in the Pt complexes and the relativistic calculation with all-electron basis sets is difficult.

How Do the 3c-2e and Agostic Interactions Determine Geometry and Bonding Nature of These Dinuclear Complexes? It is of fundamental importance to estimate how much each bonding interaction contributes to the geometry and stabilization energy of the complex. To inspect their roles, we investigated the assumed reaction shown in Figure 3. In the first step from $Pd(PH_3)_2$ **4a** to **5a**, the $Pd(PH_3)$ moiety distorts so as to form the Pd−Pd bond, where **4a**, **5a**, etc., are shown in Figure 3. Thus, the energy change (ΔE_1) by the first step corresponds to the distortion energy of the $Pd(SiH_3)(PH_3)$ moiety. In the second step, from **5a** to **6a**, the M−M bond is formed, while the 3c-2e interaction between the SiH_3 group and the M−M moiety is not formed yet in **6a**; note that the Pd−Pd−Si angle is fixed to be 90°, not to form the 3c-2e interaction. If it was not fixed, the 3c-2e interaction was formed and **5a** directly converted to **7a**. The energy change (ΔE_2) by the second step corresponds to the M−M bond energy. In the third step, from **6a** to **7a**, the Pd−Pd−Si angle is relaxed to form the 3c-2e interaction between SiH_3 and the Pd−Pd moiety. However, the agostic interaction is not formed yet in **7a**, because the rotation of the SiH_3 group is fixed so as to place the H atom at a position distant from the Pd center. The absence of the agostic interaction in **7a** will be discussed below in more detail.[31] However, the energy change (ΔE_3) of this step does not correspond to the 3c-2e interaction, as will be discussed below. In the final step from **7a** to **1a**, the rotation of the SiH_3 group is relaxed and the agostic interaction is formed in **1a**. The energy change (ΔE_4) of this step corresponds to the agostic interaction. Each geometry was optimized with the DFT method, and the energy changes by these steps were evaluated with the DFT, MP2 to MP4(SDQ), and CCSD(T) methods.

Interestingly, the dinuclear complex $Pd_2(SiH_3)_2(PH_3)_2$, **5a**, without the 3c-2e interaction, is not planar, in which the dihedral angle between the two Si−M−P planes is 76°, unlike **1a**. The reason for the nonplanar geometry is easily interpreted in terms of the four-electron repulsion between the two d_π orbitals of Pd, as follows: Because of the steric repulsion between SiH_3 and PH_3, the P−Pd−P angle is larger than 90° in **6a**. As a result, the d_π orbital becomes higher in energy by the antibonding overlap with the lone pair orbital of PH_3 and the sp^3 orbital of SiH_3, as shown in Scheme 3(A). In the planar structure, these d_{xz} and d_{xy} orbitals of one M center overlap with those of the other center to give rise to the considerably large four-electron repulsion, as shown in Scheme 3(B). In the nonplanar geometry, on the other hand, the d_{xz} and d_{xy} orbitals of the left M center are at different energies from those of the d_{xz} and d_{xy} orbitals of the right M center, respectively, as shown in Scheme 3(C), which gives rise to the smaller four-electron repulsion of these d_{xz} and d_{xy} orbitals in the nonplanar geometry than in the planar one. As a result, the nonplanar geometry is more stable than the planar one in **6a**.

Interestingly, the nonplanar **6a** changes to the planar **7a** in step 3, as shown in Figure 3. In **7a**, the three Si−H bond distances are 1.498 Å, which clearly shows that the agostic interaction is not formed in **7a**. Also, it should be noted that the Pd−Pd distance becomes considerably longer in **7a**. This result suggests that the 3c-2e interaction weakens the Pd−Pd bond probably because the 3c-2e interaction induces distortion of the Pd_2Si_2 moiety, which will be discussed below. In step 4, going to **1a** from **7a**, one of the Si−H bonds becomes considerably longer than the others, while the other geometrical changes hardly occur. These results mean that the formation of the agostic interaction is only one important change in this step.

The energy changes of these steps were evaluated with various methods, as shown in Table 1. Although the ΔE_2 value somewhat fluctuates around the MP2 and MP3 levels, the DFT, MP4(SDQ), and CCSD(T) methods present similar values, indicating that the bond energy calculated by these methods is reliable. On the other hand, the DFT-calculated ΔE_3 and ΔE_4 values are considerably smaller than the MP4(SDQ)-calculated values. Because these energy changes converge upon

Scheme 3

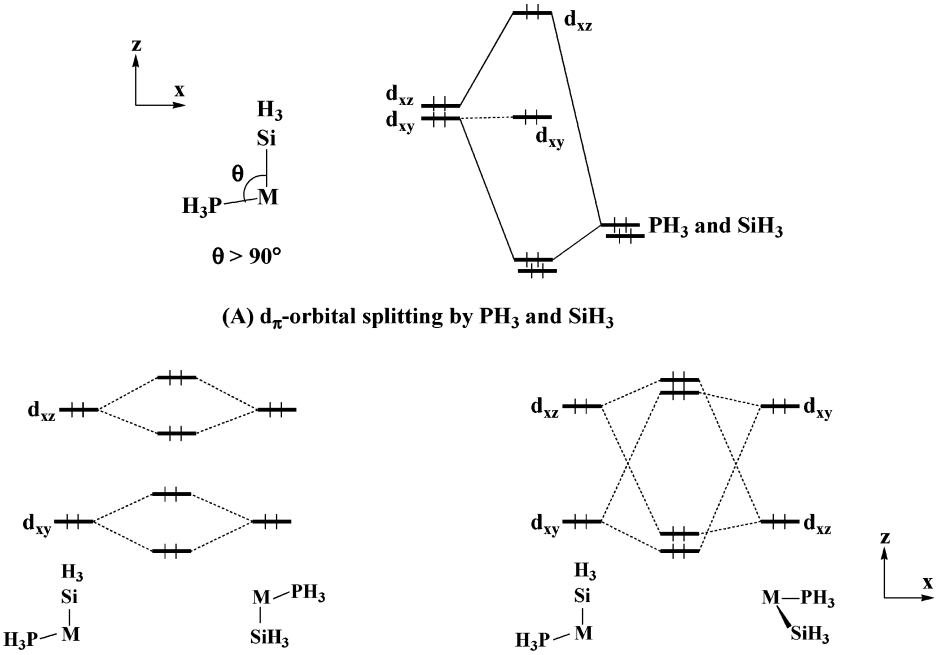

Table 1. Energy Changes[a] (in kcal/mol) along the Assumed Reaction Leading to $M_2(SiH_3)_2(PH_3)_2$ (M = Pd or Pt)

(A) M = Pd

	ΔE_1[b]	ΔE_2	ΔE_3	ΔE_4[c]	ΔE_{total}
DFT	7.0	−48.0	−48.1	−13.4	−68.5
MP2	−6.5	−60.0	−20.1	−18.2	−108.4
MP3	5.2	−42.3	−16.7	−15.5	−69.4
MP4(DQ)	−0.3	−49.4	−18.0	−16.9	−84.0
MP4(SDQ)	−3.0	−55.4	−18.3	−16.7	−93.4
CCSD(T)	5.7	−52.5	−17.8	−15.9	−80.6

(B) M = Pt

	ΔE_1[b]	ΔE_2	ΔE_3	ΔE_4[c]	ΔE_{total}
DFT	6.0	−60.4	−3.3	−27.3	−85.0
MP2	3.1	−79.1	−12.0	−40.6	−128.6
MP3	3.1	−55.7	−8.3	−35.4	−96.3
MP4(DQ)	3.1	−67.5	−9.2	−36.4	−109.9
MP4(SDQ)	3.1	−73.2	−9.5	−35.2	−114.7
CCSD(T)	3.3	−65.4	−9.2	−34.6	−105.3

[a] The negative value represents the stabilization energy and vice versa. [b] The distortion energy of two $M(SiH_3)(PH_3)$. [c] This value corresponds to the stabilization by two agostic interactions.

going from MP2 to MP4(SDQ) and CCSD(T), we will discuss the energy changes based on the CCSD(T) computational results. The ΔE_3 value (17.8 kcal/mol) is unexpectedly small. However, the ΔE_3 value does not explicitly correspond to the 3c-2e interaction, because the d_σ−d_σ bonding overlap considerably decreases in this step, as will be discussed below; in other words, this step involves the destabilization by the weakening of the d_σ−d_σ bonding interaction and the stabilization by the 3c-2e interaction. The sum of the M−M bond energy and the 3c-2e interaction is 70.3 (= ΔE_2 + ΔE_3) kcal/mol. Because the energy change (ΔE_4) in the final step corresponds to the stabilization by the agostic interaction, the strength of one agostic interaction is evaluated to be about 8 kcal/mol.

Geometry changes of the Pt system along the assumed reactions are shown in Figure 4. Several interesting differences are observed between Pt and Pd complexes. The starting $Pt(SiH_3)(PH_3)$ species is much different from the Pd analogue; the P−Pt−Si angle is not 180° but near 100° in $Pt(PH_3)(SiH_3)$. This is probably because PH_3 tends to avoid the position trans to SiH_3; remember the strong trans-influence of SiH_3.[32] The sum of the Pt−Pt bond energy and the 3c-2e interaction energy is 74.6 kcal/mol (= ΔE_2 + ΔE_3), which is not very different from that (70.3 kcal/mol) of the Pd analogue. Because it is likely that the Pt−Pt bond is stronger than the Pd−Pd bond in **1**, the 3c-2e interaction contributes more to the stabilization of **1a** than that of **1b**. On the other hand, the agostic interaction contributes much more to the stabilization of **1b** than that of **1a**. The considerably strong agostic interaction between the Si−H bond and the Pt center was previously reported in a theoretical work.[33] The difference in the agostic interaction between **1a** and **1b** is almost the same as the difference in total stabilization energy between them. In conclusion, the Pt−Pt bond and the agostic interaction of **1b** are stronger than those of **1a**, the 3c-2e interaction contributes more to the stabilization of **1a** than that of **1b**, and the agostic interaction leads to the significant difference between **1a** and **1b**.

Although extremely large differences in geometry and bonding nature were previously observed between $Pd_2(\mu\text{-}Si_2H_4)(PH_3)_4$ and $Pt_2(\mu\text{-}SiH_2)_2(PH_3)_4$,[10] the differences between **1a** and **1b** are moderate; for instance, the bonding nature is essentially the same, while the Pt−Pt bond in **6b** and the agostic interaction of **1b** are

(32) The more the (n+1)p orbital mixes into the nd orbital (n = 3 to 5), the stronger the trans-influence becomes. The nd−(n+1)p separation energy is smaller in the Pt atom than in the Pd atom, as shown by the fact that the ground state of Pt is d^9s^1 but that of Pd is d^{10}. As a result, the trans-influence in the Pt complex is stronger than that in the Pd complex.

(33) Sakaki, S.; Mizoe, N.; Sugimoto, M. *Organometallics* **1998**, *17*, 2510.

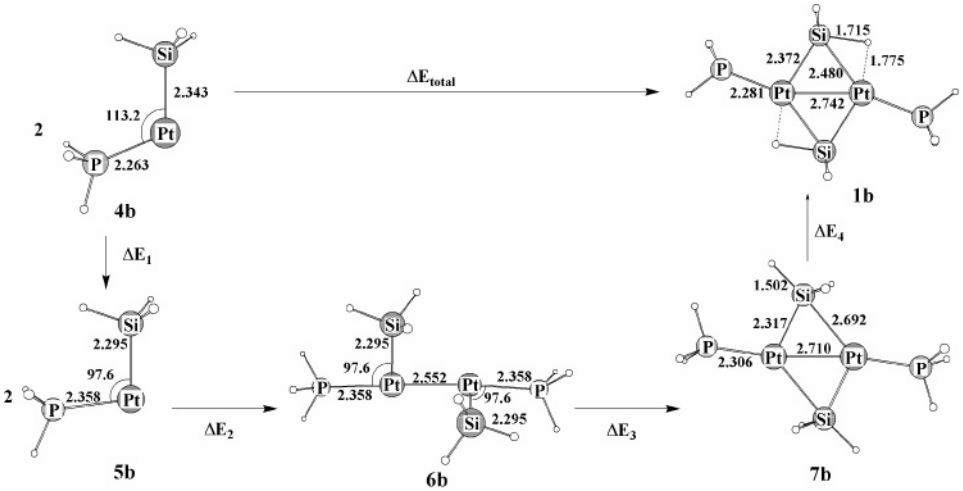

Figure 4. Geometry change along the assumed reaction from $Pt(SiH_3)(PH_3)$ to $Pt_2(SiH_3)_2(PH_3)_2$. Bond distances in angstroms and bond angles in degree.

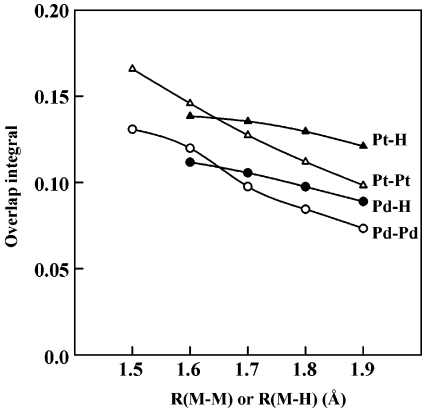

Figure 5. Overlap integrals between M and H atoms and between two M centers. Minimal basis sets, (5/5/4), (5/5/3), and (5) sets, were used for Pd, Pt, and H, respectively.

considerably stronger than those of the corresponding Pd analogues, **6a** and **1a**, respectively. These differences are interpreted in terms of the size of d orbitals, as follows: The d orbital of Pt expands more than that of Pd; actually, the radius of maximum charge density of the d orbital is 0.55 au in Pd(0) and 0.65 au in Pt(0).[34] Also, the $d_\sigma-d_\sigma$ overlap integral is considerably larger in the Pt−Pt pair than in the Pd−Pd pair, and the d_σ−1s overlap between Pt and H atoms is considerably larger than that between Pd and H atoms, as shown in Figure 5. As a result, the M−M bond and the agostic interaction are stronger in the Pt complex than in the Pd complex.

Orbital Interactions. In **5**, each M center takes a distorted T-shaped coordinate structure in which the M−M bond is involved but the 3c-2e interaction is not formed yet, as follows: The d_σ orbital interacts with that of the other M center to form the M−M σ-bonding and σ^*-antibonding orbitals, as was shown in Scheme 2, and the σ-bonding orbital is doubly occupied because the Pd(I) and Pt(I) centers have d^9 electron configuration. In the M−M σ-bonding orbital, the lone pair orbital of PH_3 and the sp^3 orbital of SiH_3 mix in a bonding way to form the M−SiH_3 and M−PH_3 coordinate bonds. Upon going to **7** from **6**, the 3c-2e interaction is formed and the geometry becomes planar, where the position of PH_3 somewhat deviates from the M−M line in **7** (see Figures 3 and 4). Because of this deviation, the P−M−Si angle is not very much different from 90° in **7**. As a result, one d_σ orbital still keeps two bonding interactions with PH_3 and SiH_3 in **7**. However, the $d_\sigma-d_\sigma$ overlap decreases by this deviation, which induces M−M bond lengthening.

Now, let us start to investigate how the 3c-2e interaction leads to the planar geometry. As discussed above, the d_σ orbitals form the $d_\sigma-d_\sigma$ bonding and $d_\sigma-d_\sigma$ antibonding orbitals, $\phi(d_\sigma-d_\sigma)$ and $*\phi(d_\sigma-d_\sigma)$. The sp^3 orbitals of two SiH_3 groups construct sp^3-sp^3 bonding and antibonding couples, $\phi(sp^3-sp^3)$ and $*\phi(sp^3-sp^3)$, as shown in Scheme 4. Its bonding couple $\phi(sp^3-sp^3)$ overlaps with the $d_\sigma-d_\sigma$ bonding couple $\phi(d_\sigma-d_\sigma)$ to afford ϕ_1 and ϕ_3. These orbital overlaps do not yield the net stabilization energy between the sp^3 orbital of SiH_3 and the M center, because both ϕ_1 and its antibonding counterpart ϕ_3 are doubly occupied. The antibonding couple $*\phi(sp^3-sp^3)$ overlaps with the $d_\sigma-d_\sigma$ antibonding couple $*\phi(d_\sigma-d_\sigma)$ to afford ϕ_2 and ϕ_4, which yields the net stabilization energy between the sp^3 orbital of SiH_3 and the M center because the ϕ_2 orbital is doubly occupied but the ϕ_4 orbital is unoccupied, as shown in Scheme 4. If the geometry is not planar, the $d_\sigma-d_\sigma$ bonding and antibonding couples do not overlap well with the sp^3 orbital of SiH_3, as shown in Scheme 5(A), because the d_σ orbital of the right M center does not interact with the sp^3 orbital of SiH_3 which is bound with the left M center. This situation is not favorable for the interaction between SiH_3 and M centers. In the planar geometry, on the other hand, the sp^3 orbital of SiH_3 that mainly interacts with the left M center somewhat overlaps with the d_σ orbital of the right M center in a bonding way, as shown in Scheme 5(B). Because of these orbital overlaps, the 3c-2e interaction is formed in the planar geometry. This is the reason that the 3c-2e interaction is responsible for the planar geometry. It is noted here that the deviation of the d_σ orbital from the M−M line is favorable for the bonding interaction between the sp^3 orbital of SiH_3 and the d_σ orbital of the right M center (Scheme 5(B)); in other words, this deviation leads to the weakening of the M−M bond, but

(34) Fraga, S.; Saxena, K. M. S.; Karwowski, J *Handbook of atomic data*; Elsevier: Amsterdam, 1976.

Scheme 4

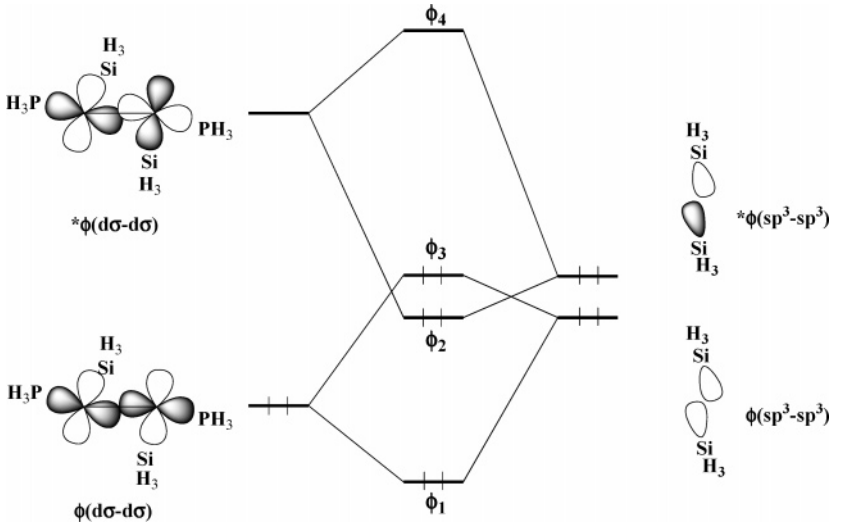

Scheme 5

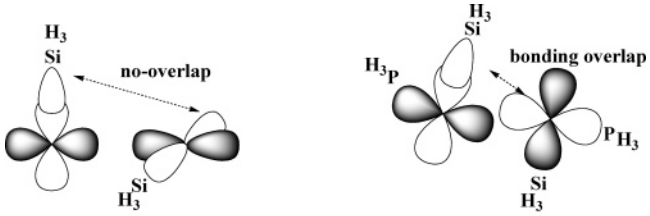

(A) no-planar geometry (B) planar geometry

its destabilization is compensated well by the stabilization energy of the 3c-2e interaction.

Finally, **7** converts to **1** with formation of the agostic interaction. Complex **1** includes all interactions discussed above. Actually, the d_σ−d_σ bonding and antibonding orbitals are observed in the HOMO−9 and LUMO, respectively, as shown in Figure 6(A). Obviously, HOMO−9 and LUMO correspond to the ϕ_1 and ϕ_4 orbitals of Scheme 4, respectively, in which the d_σ orbital somewhat deviates from the M−M line. Also, it is noted that the sp^3 orbital of SiH_3 overlaps well not only with the d_σ orbital of one M center but also with the d_σ orbital of the other M center, as discussed above. The ϕ_2 orbital is found in the HOMO−10, as shown in Figure 6(B). The d_π orbitals form bonding and antibonding molecular orbitals, as shown in Figure 6(C). Because both are doubly occupied, the d_π orbitals do not contribute at all to the stabilization energy. The agostic interaction is formed between the Si−H σ-bonding orbital and the unoccupied d orbital, in general.[35] Such interaction is observed in the HOMO−16 orbital, in which the Si−H bonding orbital overlaps with the d_σ−d_σ antibonding couple in a bonding way, as shown in Figure 6(D). In the Pt analogue, essentially the same orbitals are observed, which is shown in Supporting Information Figure S4.

These bonding pictures are consistent with the Laplacian of electron density shown in Figure 7(A). Unexpectedly, the negative value is not observed between two M centers, as reported previously.[9] This means that the Pd−Pd bond is not strong, as discussed above. The area with the largest negative value is observed between the Si^1 and Pd^1 centers, while the area with the moderately smaller negative value is observed between the Si^1 and Pd^2 centers (see Figure 7(A) for Si^1, etc.). These two areas represent the presence of the 3c-2e interaction. The considerably large negative value is observed in the area of the Si−H bond. Also, the negative value is observed in the area between the H^1 and Pd^2 centers. The presence of these areas indicates the presence of the agostic interaction. The Laplacian of electron density of the Pt analogue is omitted here, because it is essentially the same as that of the Pd complex (see Supporting Information Figure S5).

It is interesting to compare **1a** with a model silylene-bridged dinuclear complex, $[Pd_2(\mu\text{-}SiH_2)_2(PH_3)_2]^{2+}$, **8**, in which two H atoms are eliminated and pure silylene groups are involved. Interestingly, the geometry of **8** is essentially the same as that of **1a** except for the absence of two H atoms, as shown in Figure 7(B). Moreover, the Laplacian of electron density around the Si atom is similar in **1a** and **8**. These results are consistent with the above discussion that the electronic structure of the Si atom is intermediate between those of the silyl and silylene groups and that of the H atom is between those of the usual H atom and the hydride ligand. These Laplacians of electron density are consistent with the idea that **1** should be described as $M_2(\mu\text{-}\eta^2\text{-}H\cdots SiH_2)_2(PH_3)_2$.

Conclusions

Dinuclear palladium(I) and platinum(I) complexes with the composition $M_2(SiH_3)_2(PH_3)_2$ (M = Pd or Pt) were theoretically investigated with DFT, MP2 to MP4(SDQ), and CCSD(T) methods. NMR chemical shifts are interesting, as follows: The NMR chemical shift of the Si atom is intermediate between those of the typical silyl and silylene groups, and that of the H atom is intermediate between those of the usual H atom and the hydride ligand. The agostic interaction is responsible for these interesting chemical shifts. Consistent with the NMR chemical shifts, the Laplacian of electron density around the Si and M atoms is similar in $M_2(SiH_3)_2(PH_3)_2$ and the assumed μ-silylene complex, [M_2-

(35) (a) Koga, N.; Obara, S.; Morokuma, K. *J. Am. Chem. Soc.* **1984**, *106*, 4625. (b) Obara, S.; Koga, N.; Morokuma, K. *J. Organomet. Chem.* **1984**, *270*, C33. (c) Koga, N.; Obara, S.; Kitaura, K.; Morokuma, K. *J. Am. Chem. Soc.* **1985**, *107*, 7109.

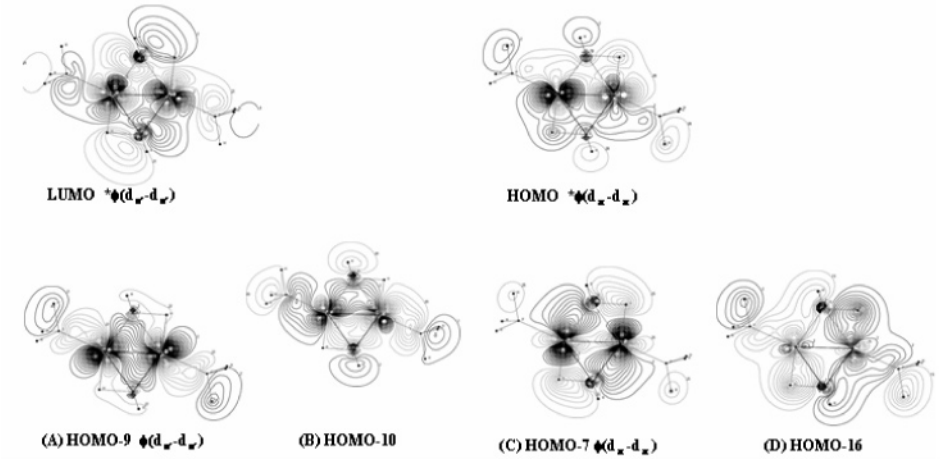

Figure 6. Contour maps (Hartree−Fock orbital) of several important molecular orbitals of $Pd_2(\mu\text{-}\eta^2\text{-}H\cdots SiH_2)_2(PH_3)_2$. Contour maps are shown with an interval of 0.01.

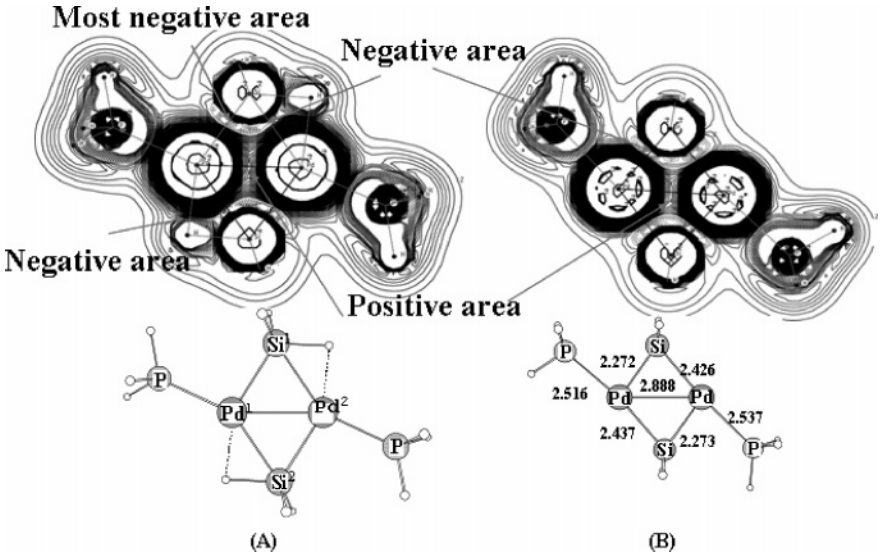

Figure 7. Laplacian of electron density of $Pd_2(\mu\text{-}\eta^2\text{-}H\cdots SiH_2)_2(PH_3)_2$ **1a** and $[Pd_2(\mu\text{-}SiH_2)_2(PH_3)_2]^{2+}$ **8**. Values are given with an interval of 0.01 (in e/au^5).

Scheme 6

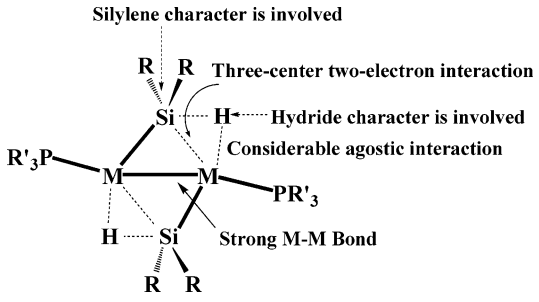

$(SiH_2)_2(PH_3)_2]^{2+}$. Thus, it is reasonably concluded that the electronic structure of the $\mu\text{-}\eta^2$-silyl-bridged group considerably shifts toward that of the hydride and μ-silylene-bridged group. This means that these complexes should be represented as $M_2(\mu\text{-}\eta^2\text{-}H\cdots SiH_2)_2(PH_3)_2$, in which the formula of $H\cdots SiH_2$ indicates that the $\mu\text{-}\eta^2\text{-}H\cdots SiH_2$ group is not a pure silyl group but possesses the characteristics of the hydride and μ-silylene group to a considerable extent. The bonding nature is schematically shown in Scheme 6.

These complexes are more stable than two $M(PH_3)(SiH_3)$ complexes by 80.6 kcal/mol for M = Pd and 105.3 kcal/mol for M = Pt, where the values calculated with the CCSD(T) method are given. The M−M bond and the three-center two-electron (3c-2e) interaction between the silyl sp^3 orbital and the M−M moiety provide energy stabilization of 70.3 and 74.6 kcal/mol for M = Pd and Pt, respectively. The planar geometry of these compounds comes from the presence of the 3c-2e interaction, which is clearly interpreted in terms of the interactions of the sp^3 orbital of the silyl group with the d_σ−d_σ bonding and antibonding couples of the M−M moiety. Because it is likely that the Pt−Pt bond is stronger than the Pd−Pd bond in **1**, the 3c-2e interaction contributes more to the stabilization of **1a** than that of **1b**. It is noted that the agostic interaction between the Si−H bond and the Pt center (17.3 kcal/mol) is much stronger than that (8.0 kcal/mol) of the Pd complex. This energy difference is similar to the total energy difference between **1a** and **1b**. These results indicate that the agostic interaction plays important roles in these dinuclear complexes; one is to induce a significantly large energy difference between **1a** and **1b**, and the other is to shift the electronic structure of SiH_3 to that of the hydride and silylene group. Although the bonding

nature of **1b** is essentially the same as that of **1a**, the Pt−Pt bond and agostic interaction of **1b** are stronger than those of **1a**, which is easily interpreted in terms that the d orbital of Pt expands more than that of Pd.

Acknowledgment. This work was in part financially supported by the Ministry of Education, Culture, Science, Technology, and Sports through Grants-in-Aid on priority areas "Reaction Control of Dynamic Complexes" (No. 420), Grants-in-Aid on the Basic area (No. 15350012), and Grants-in-Aid on Creative Science Research, and NAREGI project. All calculations were carried out on an SGI workstation and NAREGI system in the Institute for Molecular Science (Okazaki, Japan) and Pentium IV cluster systems of our laboratory.

Supporting Information Available: Complete form of ref 25. Table of basis set effects on the optimized geometry of $Pd_2(SiH_3)_2(PH_3)_2$. Table of basis set effects on the NMR chemical shift of $Pd_2(SiH_3)_2(PH_3)_2$. Figure of the optimized geometry of $Pd_2(\mu\text{-}\eta^2\text{-}SiHPh_2)_2(PMe_3)_2$. Figures of important bond angles around the Pd and Pt centers in $M_2(\mu\text{-}\eta^2\text{-}H\cdots SiH_2)_2(PH_3)_2$. Figures of optimized geometries of $Pd(H)(SiH_2)(PH_3)_2$ and $Pd(H)(SiH_3)(PH_3)_2$. Figures of contour maps of several important orbitals and the Laplacian of electron density of $Pt_2(\mu\text{-}\eta^2\text{-}H\cdots SiH_2)_2(PH_3)_2$. This material is available free of charge via the Internet at http://pubs.acs.org.

OM050292I